

# Simultaneous determination of per- and polyfluoroalkyl substances and bile acids in human serum using ultra-high-performance liquid chromatography-tandem mass spectrometry

Samira Salihović<sup>1,2</sup>, Alex M. Dickens<sup>3</sup>, Ida Schoultz<sup>1</sup>, Frida Fart<sup>1</sup>, Lisanna Sinisalu<sup>2</sup>, Tuomas Lindeman<sup>3</sup>, Jonas Halfvarson<sup>4</sup>, Matej Orešič<sup>1,3</sup>, Tuulia Hyötyläinen<sup>2\*</sup>

<sup>1</sup>School of Medical Sciences, Örebro University, 702 81 Örebro, Sweden

<sup>2</sup>School of Science and Technology, Örebro University, 702 81 Örebro, Sweden

<sup>3</sup>Turku Bioscience Centre, University of Turku and Åbo Akademi University, 20520 Turku, Finland

<sup>4</sup>Department of Gastroenterology, Faculty of Medicine and Health, Örebro University, 702 81 Örebro, Sweden

\*Corresponding author

Tuulia Hyötyläinen, PhD, Professor of Chemistry

School of Science and Technology, Örebro University, 702 81 Örebro, Sweden

Email: [tuulia.hyotylainen@oru.se](mailto:tuulia.hyotylainen@oru.se); Phone: +46 19 303487

## Abstract

There is evidence of a positive association between per- and polyfluoroalkyl substances (PFAS) and cholesterol levels in human plasma, which may be due to common reabsorption of PFAS and bile acids (BAs) in the gut. Here we report development and validation of a method that allows simultaneous, quantitative determination of PFAS and BAs in plasma, using 150  $\mu\text{l}$  or 20  $\mu\text{l}$  of sample. The method involves protein precipitation using 96-well plates. The instrumental analysis was performed with ultra-performance liquid chromatography-tandem mass spectrometry (UHPLC-MS), using reverse-phase chromatography, with the ion source operated in negative electrospray mode. The mass spectrometry analysis was carried out using multiple reaction monitoring mode. The method proved to be sensitive, robust and with sufficient linear range to allow reliable determination of both PFAS and BAs. The method detection limits were between 0.01 and 0.06  $\text{ng}\cdot\text{mL}^{-1}$  for PFAS and between 0.002 and 0.152  $\text{ng}\cdot\text{mL}^{-1}$  for BAs, with the exception of glycochenodeoxycholic acid (0.56  $\text{ng}\cdot\text{mL}^{-1}$ ). The PFAS measured showed excellent agreement with certified plasma PFAS concentrations in NIST SRM 1957 reference plasma. The method was tested on serum samples from 20 healthy individuals. In this proof-of-concept study, we identified significant associations between plasma PFAS and BA levels, which suggests that PFAS may alter the synthesis and/or uptake of BAs.

## Introduction

In clinical studies, both in metabolomics and in environmental exposure studies, the volume of sample available for analysis is often restricted. Thus, it is desirable that the analytical methods can assay multiple substance classes simultaneously, while using as small volume of sample as possible. This presents a challenge, both regarding the chemical characteristics of the compounds that can be quantitatively covered by a single extraction and/or analytical method, as well as in terms of the concentration range of said substances which can be assayed for. Whilst several methods have been developed for untargeted analyses which can simultaneously assay a large number of metabolites, it remains problematic to analyze simultaneously both specific metabolites and exogenous compounds (such as environmental pollutants) with the main challenge typically being the low concentrations of the latter.

In this study, we demonstrate the development of a targeted method for the analysis of two distinct compound classes, namely (i) endogenous bile acids (BAs) and (ii) exogenous per- and poly-fluoroalkyl substances (PFAS) in human serum or plasma. BAs are metabolites that facilitate the digestion and absorption of lipids in the small intestine. They are also important metabolic regulators involved in the maintenance of lipid and glucose homeostasis as well as in both inflammation and regeneration of the liver [1,2]. PFAS, on the other hand, are a group of man-made chemicals that have been widely used since the 1950s in both household and industrial products. PFAS also have long biological half-lives, and are readily detected in humans [3-7]. Structurally, several PFAS compounds resemble endogenous fatty acids, with fluorine substitution in place of hydrogen. Biologically, the two compound groups share some common features. It is well-known that BAs that are excreted into the intestine are reabsorbed, and similar enterohepatic circulation has been suggested for PFASs [8,9]. It has been estimated that over 90 % of perfluorooctane sulfonate (PFOS) and perfluorooctanoic acid (PFOA), the two most common PFAS, is excreted *via* bile and has to be reabsorbed, if one is to explain the long half-life of these compounds in humans [10,11]. It has also been shown that several PFAS utilize the same enterohepatic circulation as BAs [8]. Recently, the European Food Safety Authority (EFSA) reported that the positive association of PFOS and PFOA with total cholesterol serum levels, as observed in several studies, may result from a possible common reabsorption of bile acids, PFOS and PFOA from the gut and shared membrane transport pathways into the liver (<https://www.efsa.europa.eu/sites/default/files/news/efsa-contam-3503.pdf>). Interestingly, it has been hypothesized that 7-alpha-hydroxylase (CYP7A1), which catalyzes the first and rate-limiting step in the formation of BAs from cholesterol, may be down-regulated by PFAS [9,12]. This may lead to increased re-uptake of BAs, which would generate negative feedback loops *via* the farnesyl-

X-receptor and subsequently reduce their *de novo* synthesis. Indeed, PFHxS and PFOS have been shown to decrease fecal bile acid excretion [13]. Thus, current knowledge already suggests concomitant reabsorption of BAs and PFAS in the intestine and that this could play a role in the observed association between serum levels of PFAS and cholesterol. At present there is, however, limited empirical data demonstrating such a relationship.

Several methods have been developed for the quantitative determination of BAs and PFAS, using separate analytical methods [14-16]. Most of the methods include sample preparation using either (i) protein precipitation, often combined with further clean-up steps (*e.g.*, phospholipid removal), particularly for PFAS, (ii) liquid-liquid extraction, or (iii) solid-phase extraction. Such analyses are performed predominantly with various LC-MS/MS methods, typically using reversed-phase LC in combination with triple quadrupole MS in selective ion monitoring mode. For PFAS analyses, the sample volumes required for analysis are typically several hundreds of microliters, while for BAs, smaller volumes are typically sufficient.

In this study, the aim was to develop and validate a quantitative method covering both BAs and PFAS in a single analysis, minimizing the required volume of serum. The method was validated by analysis of serum samples from healthy subjects, where the associations between PFAS and BA levels were investigated.

## **Experimental**

### ***Chemicals***

Ammonium acetate (NH<sub>4</sub>Ac) was obtained from Sigma-Aldrich (St Louis, USA). Methanol (MeOH) and acetonitrile (ACN) (both HPLC grade with a purity greater than 99 %) were obtained from Fisher Scientific UK (Loughborough, United Kingdom). Acetonitrile (Optima® LC-MS grade) and formic acid (98–100 %) were purchased from Sigma Aldrich (Steinheim, Germany). The MilliQ water used to make the mobile phase was 18.2 MΩ. LC-vials and Ostro™ 96-Well Plate (25mg 1/pkg) were purchased from Waters (Waters Corporation, Milford, USA). Newborn bovine serum (New Zealand) was purchased from Sigma–Aldrich and stored frozen ( $\leq -20$  °C) until analysis. For quality assurance (QA), standard reference material serum SRM 1957 was purchased from the National Institute of Standards and Technology (NIST) at the US Department of Commerce (Washington, DC, USA). The SRM sample was stored frozen ( $\leq -20$  °C) until analysis. The quality control (QC) reference sample consisted of pooled human plasma collected from blood donors at Örebro University Hospital (Örebro, Sweden), and stored frozen ( $\leq -80$  °C) until analysis.

Abbreviations of target analytes are presented in **Table 1**. <sup>13</sup>C-labeled PFAS internal standards (IS), <sup>13</sup>C-labeled performance standards, and native calibration standards (perfluorocarboxylic acids (PFCAs) and perflurosulfonic acids (PFSAs)) were purchased from Wellington Laboratories (Guelph, Ontario, Canada). One native performance standard, 7H-dodecafluoroheptanoic acid, was purchased from ABCR (Karlsruhe, Germany). CA, CDCA, DCA, DHCA, GCA, GCDCA, LCA, TCA, TCDCA, TDCA, TDHCA, THCA, THDCA, TLCA, and TUDCA were obtained from Sigma-Aldrich (St. Luis, MO, USA), HDCA, HCA, αMCA, βMCA, ωMCA, 7-oxo-HDCA, 7-oxo-DCA, 12-oxo-LCA, TαMCA, TβMCA, TωMCA, GDHCA, GHCA, and GHDCA from Steraloids (Newport, RI, U.S.A), GLCA and GUDCA from Calbiochem (Gibbstown, NJ, U.S.A), and GDCA and UDGA from Fluka (Buchs, Switzerland). Internal standards CA-d<sub>4</sub>, LCA-d<sub>4</sub>, UDCA-d<sub>4</sub>, CDCA-d<sub>4</sub>, DCA-d<sub>4</sub>, GCA-d<sub>4</sub>, GLCA-d<sub>4</sub>, GUDCA-d<sub>4</sub> and GCDCA-d<sub>4</sub> were obtained from Qmx laboratories Ltd. (Essex, UK). All standards were prepared in methanol and stored refrigerated (4 °C).

### **Samples**

The serum samples (n=20) were from blood donors at ≥55 years of age, without any gastrointestinal disease, obtained from Örebro University Hospital. The samples were collected and registered between years 2012 and 2014. All the participants gave written consent. All serum samples were stored at -80 °C until analysis. Demographic characteristics of the study sample are shown in **ESM Table S1**.

### **Sample preparation**

The sample preparation procedure was performed as follows: all glassware and analytical syringes used were thoroughly rinsed with methanol (three times). 10 μL of PFAS internal standard mixture (c = 200 ng·μL<sup>-1</sup> in methanol) and 20 μL of BA internal standard mixture (c = 440-670 ng·μL<sup>-1</sup> in methanol) and 150 μL serum or plasma were added to a 25 mg Ostro Protein Precipitation and Phospholipid Removal 96-well plate (Waters Corporation, Milford, USA), pre-conditioned with 450 μL acetonitrile. A 450 μL aliquot of acetonitrile (containing 1 % formic acid) was added to all wells and mixed thoroughly with the sample by aspirating three times using an automated pipette. Samples were extracted using a 10" vacuum manifold for between 5–7 minutes. Aliquots of 600 μL of the eluate from each collection plate insert were then transferred to glass LC-vials and evaporated to 190 μL using nitrogen. <sup>13</sup>C-performance standards were added (10 μL of 200 ng·μL<sup>-1</sup> PFAS in methanol) as was 300 μL of 2 mM NH<sub>4</sub>AC in water. All samples and standards were ultrasonicated for 10 minutes prior to instrumental analysis to ensure homogeneity. Samples that showed precipitation were centrifuged at 9900 min<sup>-1</sup> for 10 minutes. In addition, we tested the procedure with 20 μL of serum, using the same internal standard mixtures and overall procedure,

with two exceptions: (i) a frit filter plate was used which did not remove phospholipids (96-Well Protein Precipitation Filter Plate, Sigma Aldrich), and (ii) after elution, the solvent was evaporated to dryness and the residue was dissolved in 20  $\mu\text{L}$  of a 40:60 MeOH:H<sub>2</sub>O v/v mixture containing the same <sup>13</sup>C/PFAS performance standards as the 150  $\mu\text{L}$  method.

#### ***Method calibration curve***

*Matrix-matched calibration curves for PFAS.* Matrix-matched calibration standards were made using new-born bovine serum. The standards were prepared by spiking 150  $\mu\text{L}$  newborn bovine serum with the native standard mixture resulting in an 8-point matrix matched curve ranging from 0.02 to 60 ng·mL<sup>-1</sup>, including the matrix blank. The matrix matched standards were further treated in the same way as authentic samples.

*External calibration curves for BAs.* An external calibration was used for the BAs since there is no suitable BA free plasma/serum matrix for a matrix-matched calibration. In order to ensure linearity, a calibration curve containing six calibration points (0.5-160 ng/mL), including a solvent blank, was run together with the batch of samples in this study.

#### ***LC-MS analysis***

Analyses were performed on an Acquity UPLC system coupled to a triple quadrupole mass spectrometer (Waters Corporation, Milford, USA) with an atmospheric electrospray interface operating in negative ion mode. Aliquots of 10  $\mu\text{L}$  of samples were injected into the Acquity UPLC BEH C18 2.1 mm  $\times$  100 mm, 1.7  $\mu\text{m}$  column (Waters Corporation). A trap column (PFC Isolator column, Waters Corporation) was installed between the pump and injector and used to retain fluorinated compounds originating from the HPLC system and the mobile phase. The eluent system consisted of (A) 2 mM NH<sub>4</sub>Ac in water and (B) methanol (9:1) and 2 mM NH<sub>4</sub>Ac in methanol. The gradient was programmed as follows: 0–1 min, 1 % solvent B; 1–13 min, 100 % solvent B; 13–16 min, 100 % solvent B; 16–17 min, 1 % solvent B, flow rate 0.3 ml/min. The total run time for UPLC-MS/MS analysis was 17 minutes, while the total run time for each sample injection was 20 minutes, including the reconditioning of the analytical column.

MS analysis was performed in multiple reaction monitoring (MRM) mode and experimental details of the MS/MS method are given in **ESM Table S2**. The cone and collision energies were optimized for each analyte along with the parent ion and product ion (m/z) which is shown with the abbreviations in **ESM Table S2**. Monitoring of the transitions between molecular anion [M–H]<sup>-</sup> for the PFCAs and [M]<sup>-</sup> for the PFSA and one product ion; [M–COOH]<sup>-</sup> and [FSO<sub>3</sub>]<sup>-</sup> were used for quantification of PFCAs and PFSA, respectively. Additional 1–2 product ions were monitored as qualification ions except for PFPeA and PFHxA, for which only one product ion was

monitored. For BAs, monitoring of the transitions between molecular anion  $[M-H]^-$  and one to two product ions including  $[SO_3]^-$ ,  $[taurine-H]^-$ ,  $[CH_2CHSO_3]^-$ ,  $[NH_2CH_2COO]^-$  for the conjugated BAs and  $[M-H]^-$  and  $[M-H-2H_2O]^-$  for the non-conjugated BAs.

### **Method validation**

For method validation, the following parameters were investigated: linearity, method detection limit (MDL), repeatability, accuracy and precision, recovery and matrix effect. Linearity was determined with matrix-matched standards, and plotted as relative peak areas (analyte/internal standard) versus analyte concentration.

### **Results and discussion**

The analytical method was a combination of two methods that we developed earlier for BAs and PFAS [14,17]. The main aim was to simultaneously determine both compounds classes to enable human PFAS exposure studies to investigate a potential interaction of serum/plasma PFAS and BA concentrations (Fig. 1). The method was validated for both 150  $\mu$ L and 20  $\mu$ L of serum/plasma.

#### **Validation**

*Specificity.* The method provided good chromatographic robustness, with the deviation of retention times within a time margin of  $\pm 2.5$  %. For the majority of compounds, multiple product ion fragments were monitored. In the case of the known co-eluting compounds, at least two product ions from the specific precursor ion were monitored with the requirement that the ion ratio for the secondary product ion be within 50 % variation from the selected quantification reference. For example, in the case of L-PFOS and TCDCA and TDCA (including TUDCA and THDCA) (which share the same mass of product ion  $m/z=499$  and major fragment at  $m/z=80$  and tend to co-elute) we specifically monitored two different (other than  $499>80$ ) product ions unique to the two compounds in order ensure interference-free quantitation (ESM Fig. S1).

*Linearity.* The linearity ( $R^2$ ) of the matrix-matched calibration curves ranged from 0.9995 to 0.99998 for PFAS and from 0.9909 to 0.9994 for BAs. The relative response factors (RRF) of the calibration curve ranged between 0.603-1.47 for PFAS and between 0.23-1.48 for BAs with relative standard deviation  $<15$  % for all major serum PFAS and  $<23$  % for the broad range of BAs with the exception of three BAs above 25 %: TUDCA (25 %), bMCA (33 %), and THDCA (31 %).

*Sensitivity.* MDLs were determined by calculating the mean concentrations plus three times the standard deviation in water blanks run with the sample batch ( $n=7$ ). Overall, the method performed well, giving MDLs in the range of 0.01 – 0.06  $ng\cdot mL^{-1}$  for PFAS using 150  $\mu$ L of sample. The MDLs for BAs were in the range of 0.002- 0.152  $ng\cdot mL^{-1}$ , with the exception of CA (0.1  $ng\cdot mL^{-1}$

) and GCDCA (0.56 ng·mL<sup>-1</sup>), which gave higher MDLs due to higher background noise in the water blanks. With 20 µL sample volume, the MLDs were in the range of 0.02 – 0.5 ng·mL<sup>-1</sup> for all PFAS except for PFUnDA, for which the MDL was 10 ng·mL<sup>-1</sup>. For BAs, the MLDs were in the range of 0.0025 to 1.0 ng·mL<sup>-1</sup> with the exception of wMCA and 12-oxo-LCA which had higher MDL (10 ng·mL<sup>-1</sup>).

*Accuracy and precision.* The method provided accurate data and conformed well to certified serum PFAS concentrations of NIST SRM 1957. The method was reproducible with relative standard deviations (n=10, NIST and in-house QC plasma), ranged from 2-7 % for all major plasma PFAS, with the exception of PFHpA at 24 % (**Fig. 2, ESM Table S3**). We are unaware of any NIST SRM certified values for BAs and thus performed plasma spike tests at four five levels, 0, 50, 100, 200, and 400 ng/mL of 35 BAs. The matrix spike test results demonstrated our ability to detect BAs within an error range of 20 %, with recoveries ranging from 79-106 % for most BAs (**ESM Table S4**). We also evaluated potential matrix ionization enhancement or suppression using nine internal BA standards and the PFAS performance standards at two concentrations levels; 50 and 100 ng/mL (**ESM Fig. S2**). We did not observe any deviations, other than that which is expected at 25 % difference. Similar differences were observed for the PFAS. Taken together, we can conclude that the method enables simultaneous analysis of PFAS and BAs. We also analyzed ten pooled serum samples using 20 µL of sample, and the average RSDs for both the PFAS and BA were <10% (**ESM Table S5**). However, some of the PFAS and BAs were below the MLD of the method. Overall, it is possible to reduce the sample volume, however, with some compromises in the sensitivity of the method.

#### ***PFAS and BAs in human serum***

The median concentrations of the PFAS and BAs in a series of 20 samples from healthy human individuals are shown in **Table 2**. Of the 20 measured PFAS, seven PFAS could be detected in a majority of the samples, and 19 bile acids were detected in > 70 % of the samples, and these were taken for the further data analysis. In the measured set of samples, the age or the sex did not have a significant impact on the measured concentrations.

Next, we studied the correlation between PFAS and BA concentrations. As can be seen in **Fig. 3**, specific bile acids, namely LCA, GDCA, GLCA and TLCA, showed significant associations with PFASs concentrations, with negative association between GDCA and positive associations between lithocholic acids and its two conjugates (GLCA and TLCA). The overall trend, although not reaching statistically significant in all compounds, was that the majority of circulating BAs were negatively associated with PFAS. This would suggest that the *de novo* synthesis of BAs is



downregulated, in accordance with the literature. Specifically, our findings are in line with a previous report, where several PFAS were found to suppress CYP7A1, an enzyme that controls the first and rate-limiting step in the formation of BAs from cholesterol [13]. The increased levels of LCA and its two conjugated BAs, on the other hand, could indicate any of (1) increased re-uptake of the bile acids in the gut, (2) decreased clearance from the blood, (3) increased production of the conjugated bile acids in the liver or (4) decreased de-conjugation of them by the microbiota, or any combination of these. Additionally, our results appear to suggest increased microbial formation of LCA. Indeed, PFAS exposure has been shown to cause alteration in gut microbiota, with higher exposure to PFAS associated with reduced microbiome diversity [18]. It has been shown that PFOA inhibits the function of the hepatocyte nuclear factor 4 $\alpha$  [19], which plays a central role in the regulation of BA metabolism in the liver, and is linked both with the synthesis and conjugation of primary BAs. Overall, there was a negative association between conjugated BAs and PFASs, and thus, it is more likely that the observed increase of the two conjugated BAs is related to either their re-uptake or decreased de-conjugation (**Fig. 4**). The liver clears most of the BAs *via* sodium taurocholate co-transporting polypeptide (NTCP), which has a high affinity for all conjugated BAs [20]. Interestingly, it has been demonstrated that PFBS, PFHxS, and PFOS, are also substrates for human NTCP [8].

## Conclusions

The method presented here is suitable for fast, automated analysis of PFAS and BAs from human serum, and the sample amount can be reduced to 20  $\mu$ L, however, with some loss of sensitivity. Our validation of the method demonstrated that the method is robust and accurate. Overall, our observed associations between PFAS and BAs are potentially important, as impaired BA metabolism has already been linked with type 2 diabetes (T2D), atherosclerosis and non-alcoholic fatty liver disease (NAFLD) [21]. Taurine-conjugated BAs have, for example, been found to be elevated in T2D [22]. Moreover, LCA can be cytotoxic, leading to oxidative stress, membrane damage, and colonic carcinogenesis [23], while TLCA is known to induce cholestasis by impairing biliary BA secretion [24,25]. Our preliminary findings that various PFAS have significant association with BAs supports the notion that they may play a role in the health impacts of PFAS exposure, such as the known impact of PFAS on cholesterol levels, and in metabolic pathologies such as T2D and NAFLD. Taken together, our findings warrant further investigation of the impact of both specific and mixtures of PFAS on BA metabolism, including the potential role of gut microbiota. Such studies may provide valuable insight into the pathogenesis and varying incidence of common metabolic and immune-mediated inflammatory disorders.

## Acknowledgments

This study was supported by funding from Vetenskapsrådet (to TH; grant no. 2016-05176). The authors thank Dr. Annie Von Eyken Bonafonte (University of Turku) for technical assistance and Dr. Aidan McGlinchey (Örebro University) for editing.

## Compliance with ethical standards

Study of healthy human subjects was conducted according to the Declaration of Helsinki and was approved by the regional Ethical board (Dnr. 2006/245).

## Conflict of interest

The authors declare that they have no conflict of interest.

## References

1. Haeusler RA, Astiarraga B, Camastra S, Accili D, Ferrannini E (2013) Human insulin resistance is associated with increased plasma levels of 12 $\alpha$ -hydroxylated bile acids. *Diabetes* 62 (12):4184-4191. doi:10.2337/db13-0639
2. Prawitt J, Caron S, Staels BJCDR (2011) Bile Acid Metabolism and the Pathogenesis of Type 2 Diabetes. 11 (3):160. doi:10.1007/s11892-011-0187-x
3. Kingsley SL, Walker DI, Calafat AM, Chen A, Papandonatos GD, Xu Y, Jones DP, Lanphear BP, Pennell KD, Braun JMJM (2019) Metabolomics of childhood exposure to perfluoroalkyl substances: a cross-sectional study. 15 (7):95. doi:10.1007/s11306-019-1560-z
4. Land M, de Wit CA, Bignert A, Cousins IT, Herzke D, Johansson JH, Martin JW (2018) What is the effect of phasing out long-chain per- and polyfluoroalkyl substances on the concentrations of perfluoroalkyl acids and their precursors in the environment? A systematic review. *Environmental Evidence* 7 (1):4. doi:10.1186/s13750-017-0114-y
5. Averina M, Brox J, Huber S, Furberg AS (2018) Perfluoroalkyl substances in adolescents in northern Norway: Lifestyle and dietary predictors. The Tromso study, Fit Futures 1. *Environ Int* 114:123-130. doi:10.1016/j.envint.2018.02.031
6. Sun Q, Zong G, Valvi D, Nielsen F, Coull B, Grandjean P (2018) Plasma Concentrations of Perfluoroalkyl Substances and Risk of Type 2 Diabetes: A Prospective Investigation among U.S. Women. *Environmental health perspectives* 126 (3):037001-037001. doi:10.1289/EHP2619

7. Winkens K, Vestergren R, Berger U, Cousins IT (2017) Early life exposure to per- and polyfluoroalkyl substances (PFASs): A critical review. *Emerging Contaminants* 3 (2):55-68. doi:10.1016/j.emcon.2017.05.001
8. Zhao W, Zitzow JD, Ehresman DJ, Chang S-C, Butenhoff JL, Forster J, Hagenbuch B (2015) Na<sup>+</sup>/Taurocholate Cotransporting Polypeptide and Apical Sodium-Dependent Bile Acid Transporter Are Involved in the Disposition of Perfluoroalkyl Sulfonates in Humans and Rats. *Toxicological sciences : an official journal of the Society of Toxicology* 146 (2):363-373. doi:10.1093/toxsci/kfv102
9. Chiang JY (2017) Recent advances in understanding bile acid homeostasis. *F1000Res* 6:2029-2029. doi:10.12688/f1000research.12449.1
10. Fujii Y, Niisoe T, Harada KH, Uemoto S, Ogura Y, Takenaka K, Koizumi A (2015) Toxicokinetics of perfluoroalkyl carboxylic acids with different carbon chain lengths in mice and humans. *Journal of Occupational Health* 57 (1):1-12. doi:10.1539/joh.14-0136-OA
11. Harada KH, Hashida S, Kaneko T, Takenaka K, Minata M, Inoue K, Saito N, Koizumi A (2007) Biliary excretion and cerebrospinal fluid partition of perfluorooctanoate and perfluorooctane sulfonate in humans. *Environmental Toxicology and Pharmacology* 24 (2):134-139. doi:<https://doi.org/10.1016/j.etap.2007.04.003>
12. Beggs KM, McGreal SR, McCarthy A, Gunewardena S, Lampe JN, Lau C, Apte U (2016) The role of hepatocyte nuclear factor 4-alpha in perfluorooctanoic acid- and perfluorooctanesulfonic acid-induced hepatocellular dysfunction. *Toxicology and applied pharmacology* 304:18-29. doi:10.1016/j.taap.2016.05.001
13. Bijland S, Rensen PC, Pieterman EJ, Maas AC, van der Hoorn JW, van Erk MJ, Havekes LM, Willems van Dijk K, Chang SC, Ehresman DJ, Butenhoff JL, Princen HM (2011) Perfluoroalkyl sulfonates cause alkyl chain length-dependent hepatic steatosis and hypolipidemia mainly by impairing lipoprotein production in APOE\*3-Leiden CETP mice. *Toxicol Sci* 123 (1):290-303. doi:10.1093/toxsci/kfr142
14. Jantti SE, Kivilompolo M, Ohrnberg L, Pietilainen KH, Nygren H, Oresic M, Hyotylainen T (2014) Quantitative profiling of bile acids in blood, adipose tissue, intestine, and gall bladder samples using ultra high performance liquid chromatography-tandem mass spectrometry. *Anal Bioanal Chem* 406 (30):7799-7815. doi:10.1007/s00216-014-8230-9

15. Gao K, Fu J, Xue Q, Li Y, Liang Y, Pan Y, Zhang A, Jiang G (2018) An integrated method for simultaneously determining 10 classes of per- and polyfluoroalkyl substances in one drop of human serum. *Analytica Chimica Acta* 999:76-86. doi:<https://doi.org/10.1016/j.aca.2017.10.038>
16. Yu CH, Patel B, Palencia M, Fan Z (2017) A sensitive and accurate method for the determination of perfluoroalkyl and polyfluoroalkyl substances in human serum using a high performance liquid chromatography-online solid phase extraction-tandem mass spectrometry. *Journal of Chromatography A* 1480:1-10. doi:<https://doi.org/10.1016/j.chroma.2016.11.063>
17. Salihovic S, Kärroman A, Lindström G, Lind PM, Lind L, van Bavel B (2013) A rapid method for the determination of perfluoroalkyl substances including structural isomers of perfluorooctane sulfonic acid in human serum using 96-well plates and column-switching ultra-high performance liquid chromatography tandem mass spectrometry. *Journal of Chromatography A* 1305:164-170. doi:<https://doi.org/10.1016/j.chroma.2013.07.026>
18. Iszatt N, Janssen S, Lenters V, Dahl C, Stigum H, Knight R, Mandal S, Peddada S, González A, Midtvedt T, Eggesbø M (2019) Environmental toxicants in breast milk of Norwegian mothers and gut bacteria composition and metabolites in their infants at 1 month. *Microbiome* 7 (1):34. doi:10.1186/s40168-019-0645-2
19. Buhrke T, Kruger E, Pevny S, Rossler M, Bitter K, Lampen A (2015) Perfluorooctanoic acid (PFOA) affects distinct molecular signalling pathways in human primary hepatocytes. *Toxicology* 333:53-62. doi:10.1016/j.tox.2015.04.004
20. Dawson PA (2011) Role of the intestinal bile acid transporters in bile acid and drug disposition. *Handb Exp Pharmacol* (201):169-203. doi:10.1007/978-3-642-14541-4\_4
21. de Aguiar Vallim Thomas Q, Tarling Elizabeth J, Edwards Peter A (2013) Pleiotropic Roles of Bile Acids in Metabolism. *Cell Metabolism* 17 (5):657-669. doi:<https://doi.org/10.1016/j.cmet.2013.03.013>
22. Wewalka M, Patti ME, Barbato C, Houten SM, Goldfine AB (2014) Fasting serum taurine-conjugated bile acids are elevated in type 2 diabetes and do not change with intensification of insulin. *J Clin Endocrinol Metab* 99 (4):1442-1451. doi:10.1210/jc.2013-3367
23. Barrasa JI, Olmo N, Lizarbe MA, Turnay J (2013) Bile acids in the colon, from healthy to cytotoxic molecules. *Toxicology in Vitro* 27 (2):964-977. doi:<https://doi.org/10.1016/j.tiv.2012.12.020>
24. Kakis G YI (1978) Pathogenesis of lithocholate- and tauroolithocholate-induced intrahepatic cholestasis in rats. *Gastroenterology* (4):13

25. Crocenzi FA, Mottino AD, Sánchez Pozzi EJ, Pellegrino JM, Rodríguez Garay EA, Milkiewicz P, Vore M, Coleman R, Roma MG (2003) Impaired localisation and transport function of canalicular Bsep in taurolithocholate induced cholestasis in the rat. *Gut* 52 (8):1170-1177. doi:10.1136/gut.52.8.1170
26. Zhao W, Zitzow JD, Weaver Y, Ehresman DJ, Chang S-C, Butenhoff JL, Hagenbuch B (2017) Organic Anion Transporting Polypeptides Contribute to the Disposition of Perfluoroalkyl Acids in Humans and Rats. *Toxicological sciences : an official journal of the Society of Toxicology* 156 (1):84-95. doi:10.1093/toxsci/kfw236

**Table 1.** Abbreviations of analytes measures.

Full Name	Abbreviation
Chenodeoxycholic Acid	CDCA
Cholic Acid	CA
Deoxycholic Acid	DCA
Glycochenodeoxycholic Acid	GCDCA
Glycocholic Acid	GCA
Glycodeoxycholic Acid	GDCA
Glycoursodeoxycholic Acid	GUDCA
Lithocholic Acid	LCA
Taurochenodeoxycholic Acid	TCDCA
Taurocholic Acid	TCA
Taurodeoxycholic Acid	TDCA
Taurolithocholic Acid	TLCA
Tauroursodeoxycholic Acid	TUDCA
Ursodeoxycholic Acid	UDCA
12-oxolithocholic acid	12-oxo-LCA
7-oxodeoxycholic Acid	7-oxo-DCA
7-oxohyochoolic acid	7-oxo-HCA
$\beta$ -murocholic acid	bMCA
$3\alpha,7\alpha$ -dihydroxycholestanic acid	DHCA
glycodehydrocholic acid	GDHCA
glycohyocholic acid	GHCA
glycohyodeoxycholic acid	GHDCA
glycolithocholic acid	GLCA
hyocholic acid	HCA
Hyodeoxycholic acid	HDCA
$\alpha,\beta$ -tauromurocholic acid	TabMCA
taurohyodeoxycholic acid	TDHCA
taurodeoxycholic acid	THCA
taurohyodeoxycholic acid	THDCA
$\omega$ -tauromurocholic acid	TwMCA
$\omega$ -tauromurocholic acid	waMCA
Perfluorobutanoic acid	PFBA
Perfluorobutane sulfonate	PFBS
Perfluorodecanoic acid	PFDA
Perfluorododecanoic acid	PFDoDA
Perfluorododecane sulfonate	PFDoDS
Perfluorodecane sulfonate	PFDS
Potassium Perfluoro-4-ethylcyclohexanesulfonate	PFECHS
Perfluoroheptanoic acid	PFHpA
Perfluoroheptane sulfonate	PFHpS
Perfluorohexane sulfonate	PFHxS
Perfluorononanoic acid	PFNA

Perfluorononane sulfonate	PFNS
Perfluorooctanoic acid	PFOA
Linear-Perfluorooctane sulfonate	L-PFOS
Perfluorooctane sulfonamide	PFOSA
Perfluoropentanoic acid	PFPeA
Perfluoro pentane sulfonate	PFPeS
Perfluorotetradecanoic acid	PFTDA
Perfluorotridecanoic acid	PFTTrDA
Perfluoroundecanoic acid	PFUnDA

**Table 2.** Measured concentration values from 20 healthy individuals.

	<b>Median concentration (ng/mL)</b>	<b>Min. (ng/mL)</b>	<b>Max. (ng/mL)</b>
CA	30.21	5.14	537.29
CDCA	80.11	9.87	606.25
GCA	254.40	64.07	1039.72
GCDCA	761.93	90.22	2113.96
TCDCa	97.92	11.39	371.25
12-oxo-LCA	13.26	2.45	34.82
DCA	240.82	0.01	737.10
HDCA	86.99	8.48	498.08
LCA	6.73	0.00	21.96
UDCA	30.12	16.76	194.31
GDCA	295.31	0.14	2154.80
GHCA	5.66	2.50	15.89
GHDCA	7.60	0.05	46.41
GLCA	20.32	4.25	141.00
GUDCA	34.94	4.49	264.67
TabMCA	1.97	0.00	17.94
TDCA	35.69	2.37	113.93
THCA	1.60	0.00	7.71
TLCA	3.19	1.09	12.60
PFHxS	0.78	0.07	6.18
PFOA	1.42	0.15	3.48
PFNA	0.76	0.06	2.03
L-PFOS	4.20	0.44	16.69
PFDA	0.37	0.04	0.84
PFUnDA	0.39	0.06	0.91
PFTTrDA	0.08	0.01	0.20



## Figure legends

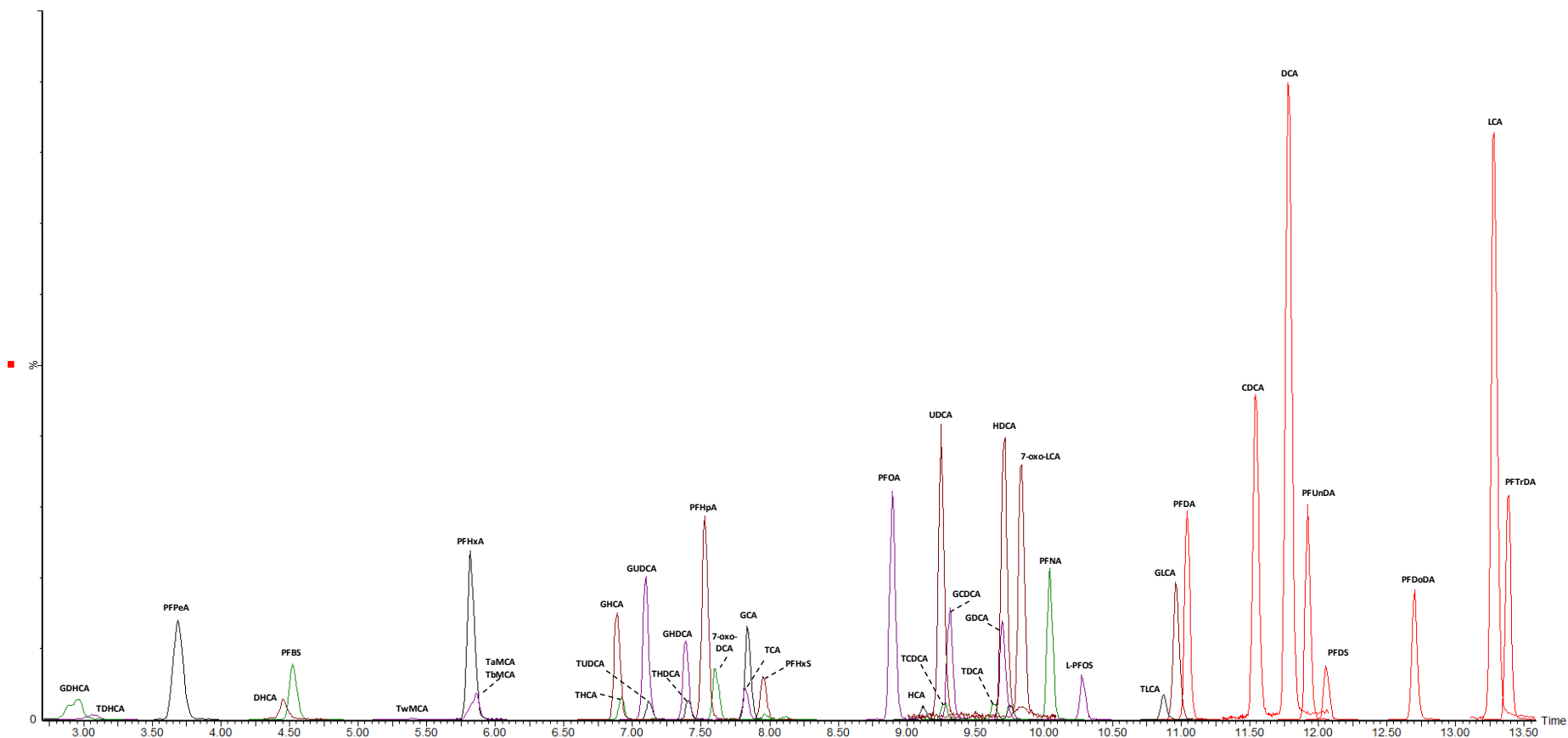
**Fig. 1.** Example total ion chromatogram of target analytes in elution order, in accordance with **ESM Table S2**.

**Fig. 2.** Conformity of measured PFAS concentration with certified values in NIST SRM 1957.

**Fig. 3.** Correlation plot of PFAS and BAs (Spearman correlation), significance of the correlations is marked (\*\* $p < 0.01$ , \* $p < 0.05$  and \*  $p < 0.1$ ).

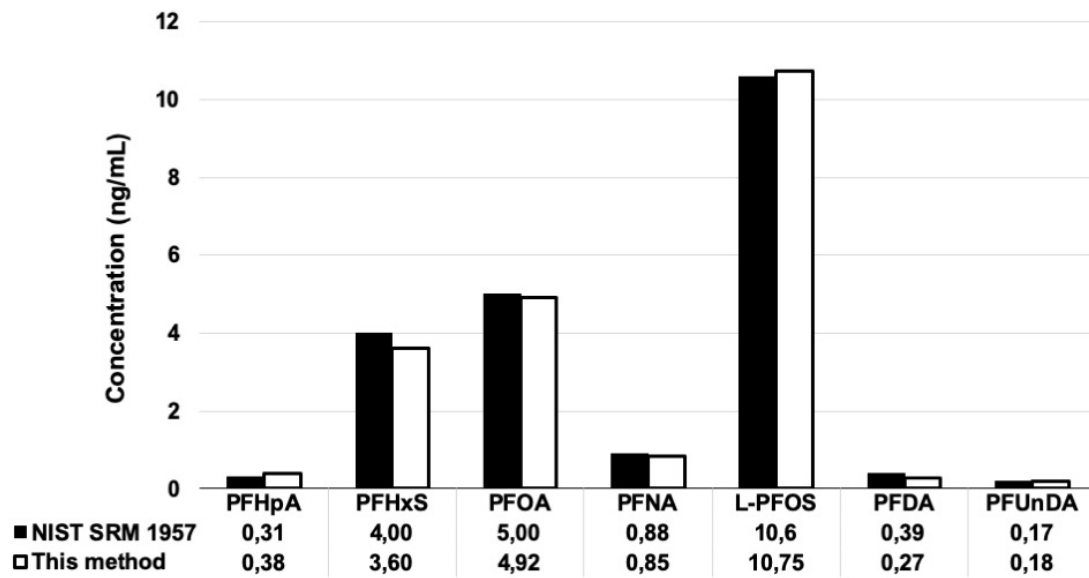
**Fig. 4.** The enterohepatic circulation of bile acids. Primary bile acids (CA, cholic acid; CDCA, chenodeoxycholic acid) are synthesized from cholesterol in the liver, with the first step controlled primarily via the action of cholesterol  $7\alpha$ -hydroxylase (CYP7A1) which is downregulated by PFAS. Before the primary bile acids are secreted into the canalicular lumen they are conjugated with either of the amino acids, glycine or taurine. HNF4 $\alpha$  can regulate the genes involved in BA biosynthesis, including hydroxylation and side chain  $\beta$ -oxidation of cholesterol in vivo. Once in the large intestine, bacterial flora catalyzes their biotransformation into secondary bile acids: deoxycholic acid (DCA) and lithocholic acid (LCA). Ursodeoxycholic acid (UDCA) derives from epimerization of CDCA. From the colon, around 95% are reabsorbed into the distal ileum. The absorbed primary and secondary bile acids and salts are transported back to the liver where most of the conjugated BAs as well as PFAS are actively transported into hepatocytes by sodium sodium (Na<sup>+</sup>)-taurocholate co-transporting polypeptide (NTCP). Once in the liver the BAs are reconjugated and then re-secreted together with newly synthesized bile salts. Red arrows: positive association with PFAS, blue arrow negative association with PFAS. The impact on CYP7A1, HNF4 $\alpha$  and NTCP are based on literature [12,8,26,19].

1 **FIGURE 1**



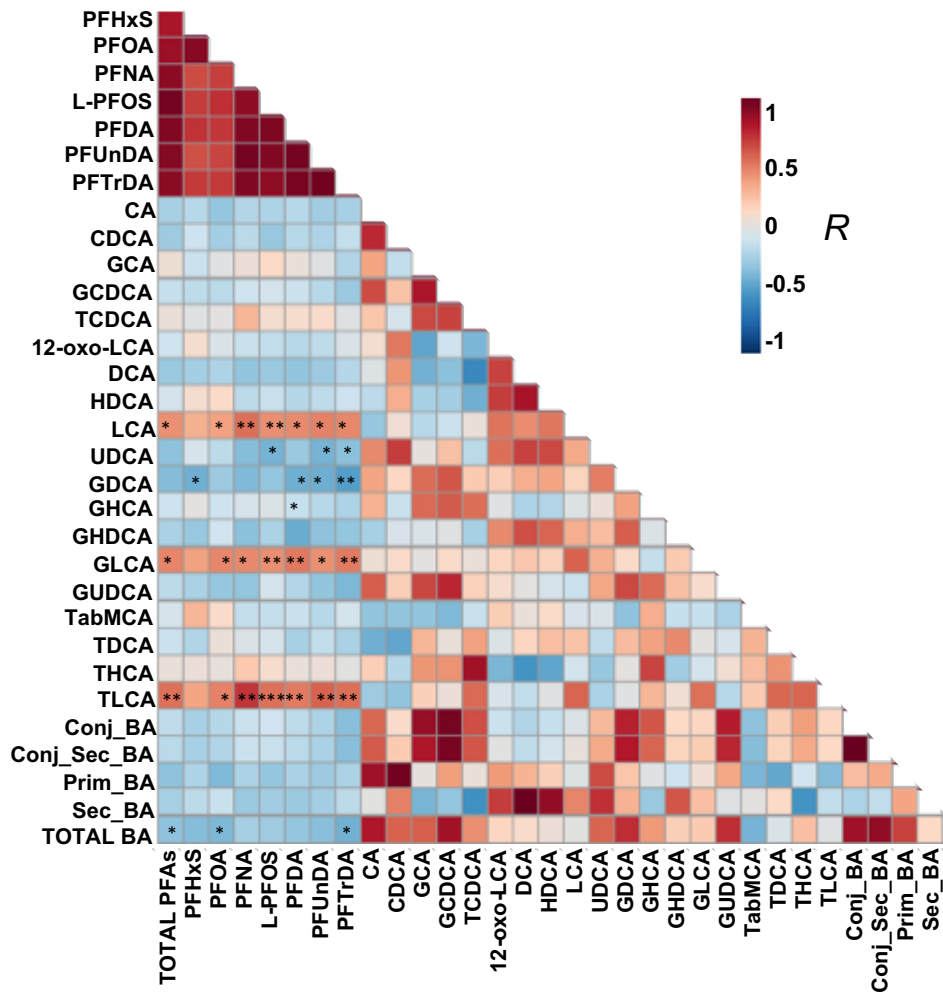
2

3 FIGURE 2



4

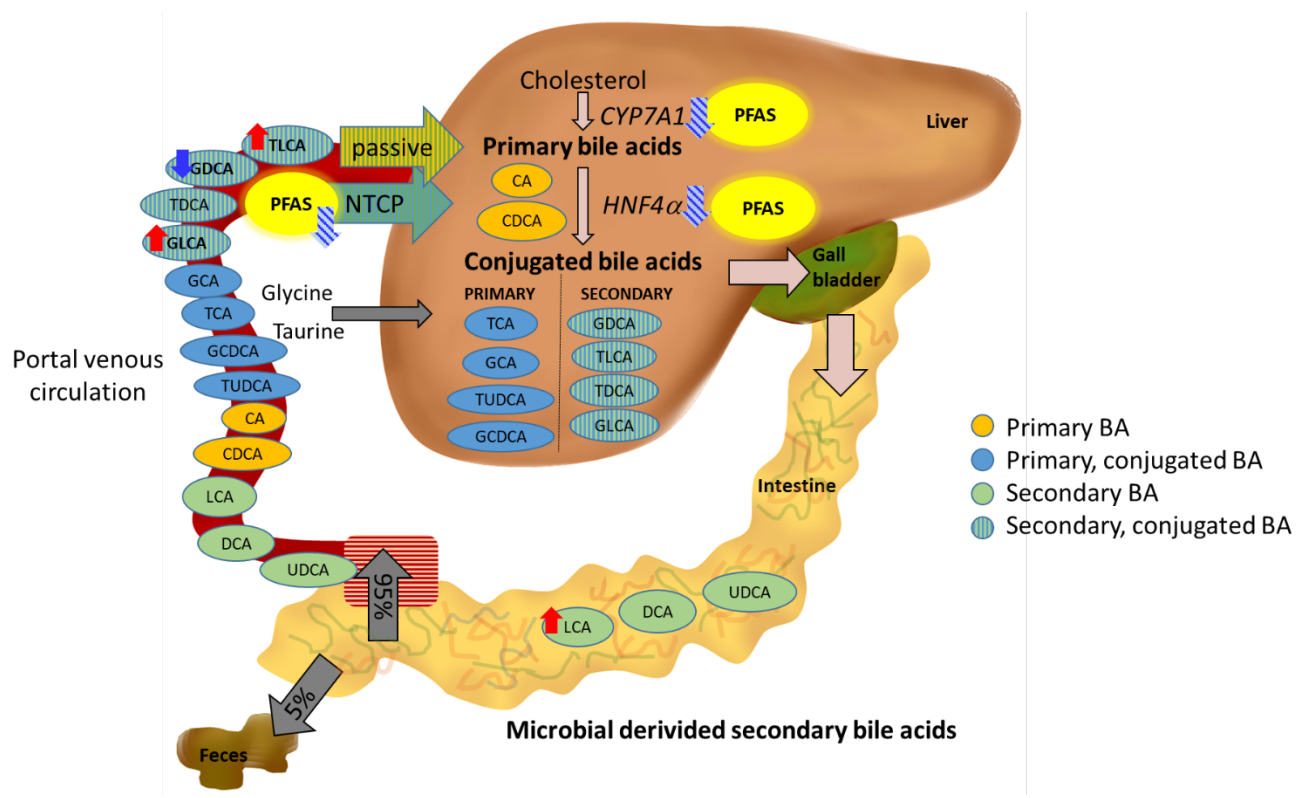
5 FIGURE 3



6

7

8 FIGURE 4



9

10



12 **ESM Table S1.** Demographic characteristics of the study population (n=20).

<b>Parameter</b>	<b>Median (range)</b>
<b>Age (years)</b>	58.5 (55-69)
<b>Sex</b>	13/7(Male/Female)

13

14 **ESM Table S2.** Acquisition parameters including the list or targets compounds ordered by retention time.

	Target analytes	Abbreviation	Retention time	Precursor Ion (m/z)	Product Ion (m/z)			Cone (V)	Collision (eV)		
					1	2	3		1	2	3
1	Glycodehydrocholic acid	GDHCA	2.97	458.1	74.0	348.1	388.1	52.0	32.0	28.0	28.0
2	Taurodehydrocholic acid	TDHCA	3.09	508.1	80.0	106.9	124.0	80.0	66.0	54.0	55.0
3	Perfluoropentanoic acid	PFPeA	3.70	262.7	68.9	219.0	–	20.0	33.0	8.0	–
4	Dihydroxycholestanic acid	DHCA	4.45	401.1	215.0	249.0	331.0	74.0	32.0	30.0	24.0
5	Perfluorobutane sulfonate	PFBS	4.53	298.9	80.0	98.9	–	20.0	26.0	26.0	–
6	Tauro-omega-muricholic acid	TwMCA	5.38	514.2	80.0	106.9	123.9	70.0	50.0	44.0	42.0
7	Perfluorohexanoic acid	PFHxA	5.82	312.8	68.9	119.0	269.0	20.0	40.0	26.0	9.0
8	Tauro-alpha-muricholic acid	TaMCA	5.81	514.2	80.0	106.9	123.9	70.0	50.0	44.0	42.0
9	Tauro-beta-muricholic acid	TbMCA	5.87	514.2	80.0	106.9	123.9	70.0	50.0	44.0	42.0
10	Glycohyocholic acid	GHCA	6.88	464.2	74.0	–	–	52.0	32.0	–	–
11	Trihydroxycholestanic acid	THCA	6.92	514.2	80.0	106.9	123.9	60.0	50.0	44.0	42.0
12	Glycoursodeoxycholic acid	GUDCA	7.10	448.2	74.0	–	–	52.0	32.0	–	–
13	Tauroursodeoxycholic acid	TUDCA	7.11	498.2	80.0	106.9	123.9	70.0	50.0	46.0	45.0
14	Glycohyodeoxycholic acid	GHDCA	7.39	448.2	74.0	–	–	52.0	32.0	–	–
15	Taurohyodeoxycholic acid	THDCA	7.40	498.2	80.0	106.9	123.9	70.0	50.0	46.0	45.0
16	Perfluoroheptanoic acid	PFHpA	7.53	363.0	169.0	319.0	–	20.0	16.0	10.0	–
17	7-oxo-deoxycholic acid	7-oxo-DCA	7.61	405.2	123.0	–	–	77.0	36.0	–	–
18	Taurocholic acid	TCA	7.82	514.2	80.0	106.9	123.9	70.0	50.0	44.0	42.0
19	Glycocholic acid	GCA	7.84	464.2	74.0	–	–	52.0	32.0	–	–
20	7-oxo-hyocholic acid	7-oxo-HCA	7.88	405.2	375.3	–	–	77.0	26.0	–	–
21	Perfluorohexane sulfonate	PFHxS	7.95	398.9	80.0	98.9	119.0	20.0	34.0	30.0	28.0
22	omega/alpha-Muricholic acid	w/a-MCA	7.97	407.2	371.2	–	–	70.0	36.0	–	–
23	beta-Muricholic acid	b-MCA	8.12	407.2	371.2	–	–	70.0	36.0	–	–
24	Perfluorooctanoic acid	PFOA	8.89	413.0	169.0	219.0	369.0	20.0	18.0	14.0	10.0
25	Hyocholic acid	HCA	9.11	407.1	389.2	–	–	76.0	32.0	–	–



26	Ursodeoxycholic acid	UDCA	9.25	391.1	391.1	-	-	45.0	2.0	-	-
27	Taurochenodeoxycholic acid	TCDCA	9.26	498.2	80.0	106.9	123.9	70.0	50.0	50.0	50.0
28	Glychenodeoxycholic acid	GCDCA	9.31	448.2	74.0	-	-	52.0	32.0	-	-
29	Taurodeoxycholic acid	TDCA	9.63	498.2	80.0	106.9	123.9	70.0	50.0	50.0	-
30	Glycodeoxycholic acid	GDCA	9.70	448.2	74.0	-	-	52.0	32.0	-	-
31	Hyodeoxycholic acid	HDCA	9.72	391.1	391.1	-	-	45.0	2.0	-	-
32	Cholic acid	CA	9.74	407.2	343.2	-	-	76.0	32.0	-	-
33	12-oxo-lithocholic acid	12-oxo-LCA	9.84	389.1	389.1	-	-	45.0	2.0	-	-
34	Perfluorononanoic acid	PFNA	10.04	463.0	219.0	419.0	-	20.0	18.0	12.0	-
35	Linear-perfluorooctane sulfonate	L-PFOS	10.27	499.0	80.0	99.0	169.0	20.0	44.0	38.0	34.0
36	Taurolithocholic acid	TLCA	10.87	482.2	80.0	106.9	123.9	80.0	60.0	54.0	44.0
37	Glycolithocholic acid	GLCA	10.96	432.2	73.9	-	-	32.0	32.0	-	-
38	Chenodeoxycholic acid	CDCA	11.54	391.1	391.1	-	-	45.0	4.0	-	-
39	Deoxycholic acid	DCA	11.78	391.1	391.1	-	-	45.0	4.0	-	-
40	Perfluorodecanoic acid	PFDA	11.04	513.0	219.0	469.0	-	20.0	18.0	11.0	-
41	Perfluoroundecanoic acid	PFUnDA	11.92	563.0	269.0	519.0	-	20.0	18.0	12.0	-
42	Perfluorodecane sulfonate	PFDS	12.05	599.0	80.0	98.9	-	20.0	58.0	42.0	-
43	Perfluorododecanoic acid	PFDoDA	12.70	613.0	169.0	569.0	-	34.0	14.0	-	-
44	Lithocholic acid	LCA	13.28	375.1	375.1	-	-	47.0	4.0	-	-
45	Perfluorotridecanoic acid	PFTTrDA	13.39	662.9	169.0	619.0	-	20.0	26.0	14.0	-
Internal standards											
46	[13C4]- Perfluoropentanoic acid	13C4-PFPeA	3.68	266.0	222.0	-	-	20.0	8.0	-	-
47	[13C3]- Perfluoropentanoic acid	13C3-PFBS	4.51	301.9	98.9	-	-	20.0	26.0	-	-
48	[13C2]- Perfluorohexanoic acid	13C2-PFHxA	5.82	315.0	270.0	-	-	20.0	9.0	-	-
49	[D4]- Glyoursodeoxycholic acid	D4-GUDCA	7.09	452.2	74.0	-	-	52.0	32.0	-	-
50	[13C4]- perfluoroheptanoic acid	13C4-PFHpA	7.53	367.0	322.0	-	-	20.0	10.0	-	-
51	[D4]- Taurocholic acid	D4-TCA	7.82	518.2	123.9	-	-	70.0	42.0	-	-
52	[D4]- Glycocholic acid	D4-GCA	7.83	468.2	74.0	-	-	52.0	32.0	-	-
53	[18O3]- perfluorohexane sulfonate	13O3-NaPFHxS	7.95	402.9	102.9	-	-	20.0	30.0	-	-

54	[13C4]- perfluorooctanoic acid	13C4-PFOA	8.89	417.0	372.0	-	-	20.0	10.0	-	-
55	[D4]- Ursodeoxycholic acid	D4-UDCA	9.24	395.1	395.1	-	-	45.0	2.0	-	-
56	[D4]- Glycochenodeoxycholic acid	D4-GCDCA	9.30	452.2	74.0	-	-	52.0	32.0	-	-
57	[D4]- Cholic acid	D4-CA	9.74	411.2	347.2	-	-	84.0	32.0	-	-
58	[13C5]- perfluorononanoic acid	13C5-PFNA	10.04	468.0	423.0	-	-	20.0	12.0	-	-
59	[13C4]- perfluorooctane sulfonate	13C4-NaPFOS	10.27	503.0	99.0	-	-	20.0	38.0	-	-
60	[D4]- Glycolithocholic acid	D4-GLCA	10.96	436.2	73.9	-	-	32.0	32.0	-	-
61	[13C2]- perfluorodecanoic acid	13C2-PFDA	11.04	515.0	470.0	-	-	20.0	11.0	-	-
62	[D4]- Chenodeoxycholic acid	D4-CDCA	11.53	395.1	395.1	-	-	45.0	4.0	-	-
63	[D4]- Deoxycholic acid	D4-DCA	11.78	395.1	395.1	-	-	45.0	4.0	-	-
64	[13C2]- perfluoroundecanoic acid	13C2-PFUnDA	11.92	565.0	520.0	-	-	20.0	12.0	-	-
65	[13C2]- perfluorododecanoic acid	13C2-PFDoDA	12.70	615.0	570.0	-	-	34.0	14.0	-	-
66	[D4]- Lithocholic acid	D4-LCA	13.26	379.1	379.1	-	-	47.0	4.0	-	-
Performance standards											
67	[13C5]- perfluoropentanoic acid	13C5-PFPeA	3.68	268.0	223.0	-	-	20.0	8.0	-	-
68	[13C5]- perfluorohexanoic acid	13C5-PFHxA	5.81	318.0	273.0	-	-	20.0	9.0	-	-
69	[13C4]- perfluorohexane sulfonate	13C4-NaPFHxS	7.95	401.9	98.9	-	-	20.0	30.0	-	-
70	[13C8]- perfluorooctanoic acid	13C8-PFOA	8.89	421.0	376.0	-	-	20.0	10.0	-	-
71	[13C9]- perfluorononanoic acid	13C6-PFNA	10.04	472.0	427.0	-	-	19.0	12.0	-	-
72	[13C8]- perfluorooctane sulfonate	13C8-NaPFOS	10.27	507.0	99.0	-	-	20.0	38.0	-	-
73	[13C6]- perfluorodecanoic acid	13C6-PFDA	11.04	519.0	474.0	-	-	20.0	11.0	-	-
74	[13C7]- perfluoroundecanoic acid	13C7-PFUnDA	11.92	570.0	525.0	-	-	20.0	12.0	-	-

16 **ESM Table S3.** Recovery mean, recovery range and RSD of the internal standards in the NIST  
 17 SRM 1957 and QC plasma samples.

Internal standards (PFAS)	NIST SRM 1957 (n=4)			QC plasma (n=7)		
	Mean (%)	Recovery range (%)	RSD	Mean (%)	Recovery range (%)	RSD
<sup>13</sup> C-PFHPeA	119	99.6-120	13.7	111	94.6-127	9.93
<sup>13</sup> C-PFHxA	111	94.9-116	8.15	106	93.3-122	6.67
<sup>13</sup> C-PFHpA	118	101-116	6.28	109	81.9-131	13.3
<sup>13</sup> C-PFHxS	110	89.5-119	11.6	104	92.3-124	7.55
<sup>13</sup> C-PFOA	110	93.0-115	8.74	106	93.0-121	8.42
<sup>13</sup> C-PFNA	114	92.4-114	9.28	106	91.5-127	7.97
<sup>13</sup> C-L-PFOS	116	87.0-116	14.3	107	90.7-128	7.76
<sup>13</sup> C-PFDA	117	81.5-117	14.7	102	88.8-132	9.53
<sup>13</sup> C-PFUnDA	119	61.4-117	25.9	90.6	87.2-138	12.1

18

19

20 **ESM Table S4.** Recovery mean, recovery range and RSD of the bile acids in NIST SRM 1957  
 21 and QC plasma samples.

Internal standards (BA)	NIST SRM 1957 (n=4)			QC plasma (n=7)		
	Mean (%)	Recovery range (%)	RSD	Mean (%)	Recovery range (%)	RSD
D4-CA	63.9	53.7-83	21%	48.0	37.2-83.1	30%
D4-GCA	52.0	41.4-67.2	21%	55.7	48.8-72.9	13%
D4-GUDCA	70.3	60.2-89.4	19%	70.9	62.2-90.8	13%
D4-GCDCA	48.5	40-61.6	19%	53.4	46.3-77.5	19%
D4-UDCA	100.0	88.5-122.8	16%	75.2	69.8-82.6	6%
D4-CDCA	104.9	87.9-136.1	21%	59.3	50.5-70.5	11%
D4-DCA	81.9	69.2-101.9	17%	52.9	45-65	13%
D4-GLCA	40.2	35.7-48	14%	46.6	39-68	20%
D4-LCA	81.1	67-89.1	12%	74.8	68-90.3	11%

22

23 <sup>1</sup>also applied for HCA

24 <sup>2</sup>also applied for GHCA

25

26

27 **ESM Table S5.** Linear range, limits of detection, average concentration and RSD of the PFAS  
 28 and BA in QC plasma samples (n= 10) using 20 µl sample volume.

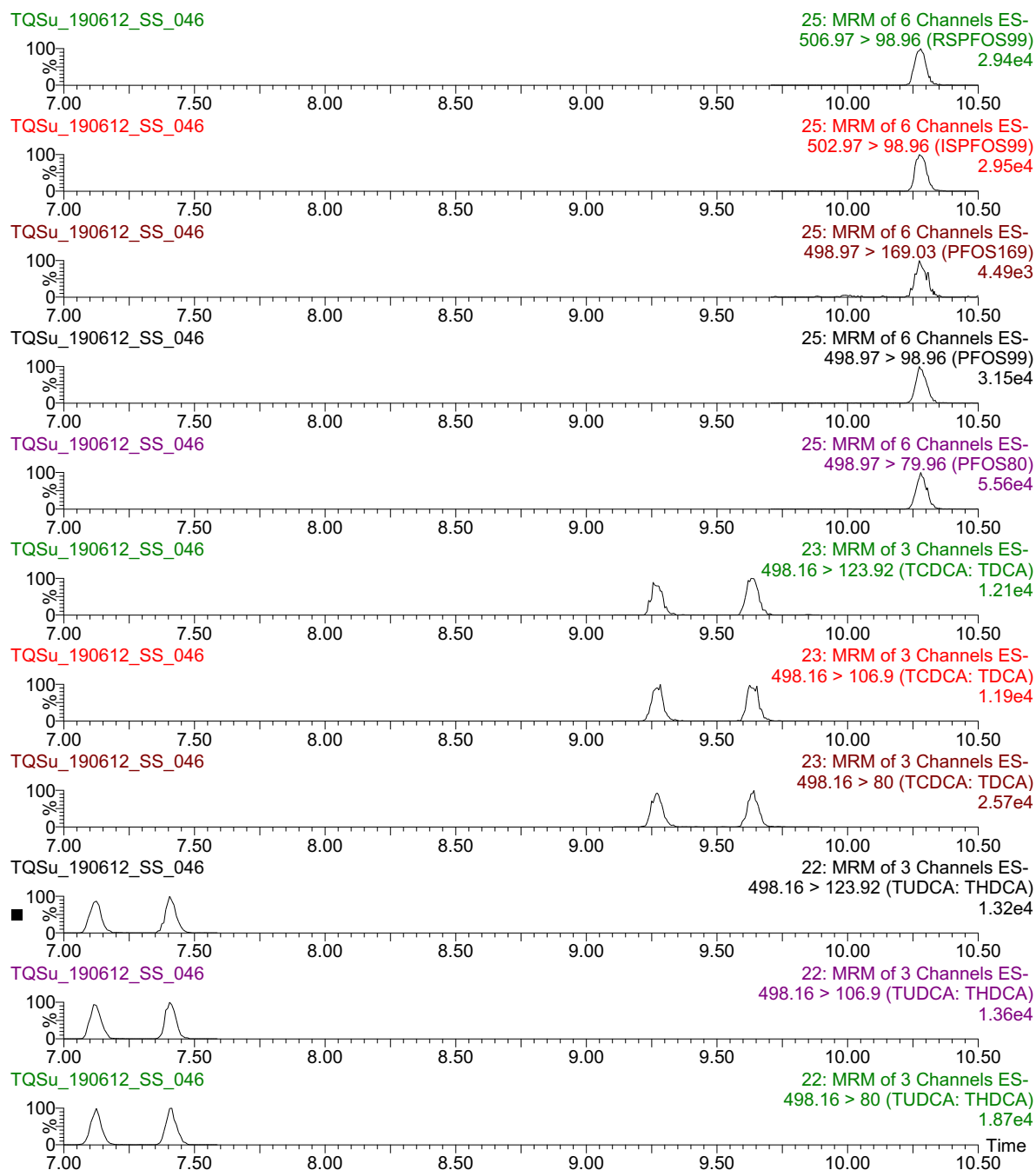
Analyte	r	LLOQ	ULOQ	Average concentration	%RSD
TDHCA	0.9989	0.0025	300	2.07	32.06
TaMCA	0.9982	0.5	300	12.91	6.5
TwMCA	0.9982	1	600		
TbMCA	0.9966	0.25	600	16.76	7.98
GDHCA	0.9991	0.25	600	nd	n/a
THCA	0.9985	0.25	600	25.22	4.52
TUDCA	0.9989	0.25	600	19.74	3.72
7-OXO-DCA	0.999	0.025	600	2.85	43.2
7-OXO-HDCA	0.9986	0.25	600	nd	n/a
aMCA	0.9968	0.5	600	nd	n/a
bMCA	0.9948	1	600	nd	n/a
CA	0.9959	0.25	600	30.62	7.23
CDCA	0.9992	1	600	49.23	5.09
DCA	0.9991	0.025	600	16.55	10.51
DHCA	0.9897	0.5	600	nd	n/a
GCA	0.9992	0.0025	600	317.9	2.49
GCDCA	0.9991	0.0025	600	1004.2	2.02
GDCA	n/a	n/a	n/a		
GHCA	0.9986	0.025	600	34.31	8.45
GHDCA	0.9986	0.0025	600	86.57	4.15
GLCA	0.9998	0.0025	600	3.56	31.3
GUDCA	0.9984	0.0025	600	88.36	3.46
HCA	0.9973	0.25	300	11.31	10.77
HDCA	0.9987	0.5	600	nd	n/a
LCA	0.9989	0.5	300	nd	n/a
TCA	0.9985	1	600	97.97	3.63
TCDCA	0.9997	0.0025	600	380.3	3.55
TDCA	0.9996	0.25	600	12.2	4.96
THDCA	0.9981	0.25	600	14.49	6.8
TLCA	0.993	0.25	600	nd	n/a
UDCA	0.9993	0.25	600	28.52	3.71
wMCA	0.98	10	600	nd	n/a
12-OXO-LCA	0.9982	10	600	nd	n/a
PFBuS	0.9987	0.025	200	nd	n/a
PFDA	0.53	n/a	n/a	n/a	n/a
PFDoDA	0.9995	0.5	200	nd	n/a
PFDS	0.9978	0.5	200	nd	n/a
PFHpA	0.9996	0.025	200	nd	n/a

PFHxA	0.995	0.025	200	nd	n/a
PFHxS	0.9985	0.25	200	nd	n/a
PFNA	0.9993	0.025	200	nd	n/a
PFOA	0.999	0.25	200	n/a*	n/a
PFOS	0.9993	0.025	200	0.53	3.04
PFOSA	0.9997	0.5	200	0.07	7.4
PFPeA	0.9975	0.025	100	nd	n/a
PFTTrDA	0.9975	0.5	200	1.57	0.92
PFUnDA	0.9991	10	200	nd	n/a

29

\*High background level in the blanks

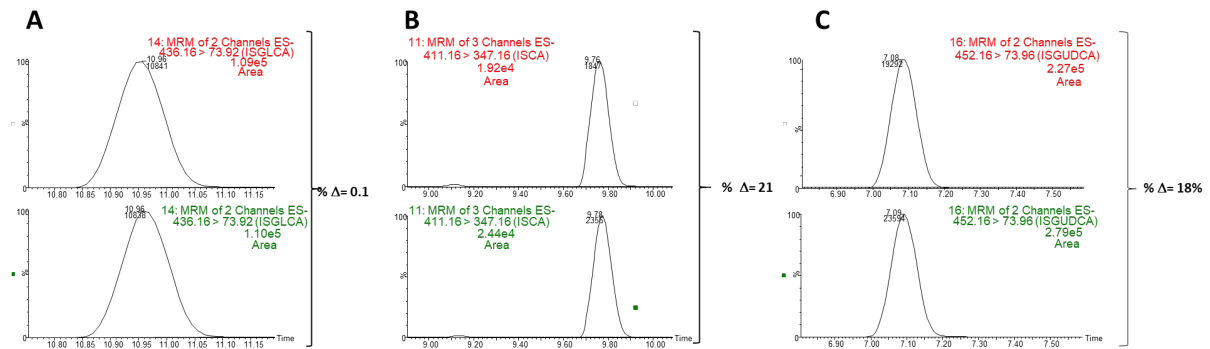
30 **ESM Fig. S1.** Some BAs such as TCDCA and TDCA as well as TUDCA and THDCA undergoes  
 31 the same transition (499 > 80 m/z) and also readily to co-elute with L-PFOS. Chromatographic  
 32 separation and multiple product ions were selected to reduce potential interferences of selected  
 33 BAs with L-PFOS.



34

35

36 **ESM Fig. S2.** Matrix suppression for (A) d<sub>4</sub>-GLCA, (B) d<sub>4</sub>-GCA and (C) d<sub>4</sub>-GUDCA, with ISTD  
37 added before (upper panels) and after sample clean-up (lower panels) and the deviation between  
38 the peak areas.



39

40